Università di Pisa
Dipartimento di Informatica

Technical Report: TR-02-17

SPECT imaging reconstruction through discretization on a polar grid

R. Bevilacqua E. Bozzo O. Menchi

November 28, 2002

ADDRESS: Corso Italia 40, 56125 Pisa, Italy. TEL: +39 050 2212700 FAX: +39 050 2212726

SPECT imaging reconstruction through discretization on a polar grid

R. Bevilacqua E. Bozzo O. Menchi

November 28, 2002

Abstract

The problem of reconstructing a two-dimensional tomographic medical image is considered. The emission function $f(P)$ is defined on a plane circular domain Ω and has to be reconstructed from data collected by SPECT. In this paper the natural pixel discretization approach is used, for which suitable basis functions must be chosen. We show that by choosing the basis on a polar grid a highly structured coefficient matrix can be obtained. Numerical experimentation validates the efficiency of this approach.

1 Introduction

The problem of reconstructing a two-dimensional tomographic medical image is considered. In most cases medical imaging involves the reconstruction of two-dimensional slices of a three dimensional body. These separate reconstructions can be used to build a spatial representation of the object. This is the case [5] of the so-called (2D+1) model for SPECT (Single Photon Emission Computed Tomography), an emission tomography technique which measures the radiation emitted by a radioactive tracer injected in the patient's body. A planar vertical array of detectors placed on a turning device measures the radiation which passes through a collimator, then only the photons arriving along the direction perpendicular to the detector itself are counted. These measures are made in correspondence of a discrete set of angles equally spaced in 2π. In the two-dimensional case here considered the emission function $f(P)$ is defined on a plane circular domain Ω and has to be reconstructed from data collected by aligned detectors rotating around the center of Ω. In general this kind of problems are solved by using some discretization technique. Here we refer to the *natural pixel discretization* approach described in [4, 6]. This approach leads to the solution of a strongly ill-conditioned linear system, whose coefficient matrix depends on the geometric response of the device and on nonuniform attenuation effects varying from patient to patient. Here we assume that, as is customary in cerebral SPECT reconstruction, that uniform attenuation holds. Under this hypothesis only the data collected by the device depend on the patient.

The patient data are contaminated by noise due to the acquisition process, hence a regularized solution is sought. In this setting the technique suggested in [4] expresses the solution as a linear combination of linearly independent functions defined on Ω and obtains the coefficients of the combination by solving a linear system of normal equations. The matrix of the system is highly structured matrix, i.e. is block circulant. The structure can be exploited in such a way that considerable part of the computation is done once for all by reducing the matrix into a block diagonal form through the use of the Fourier transform. The remaining part of the computation is then performed for each new set of patient data. However this approach has a drawback: the increase of the ill-conditioning implicitly due to the use of normal equations.

We show here that by choosing the basis functions on a suitable polar grid we obtain directly, without setting up the normal equations, a nonsymmetric square block circulant matrix. With this approach we retain the structure properties of the matrix without the ill-conditioning increase. The matrix is reduced into a block diagonal form by the Fourier transform. The original system is thus divided into smaller systems, which are solved in the regularized way by applying truncated SVD. Also the computation of the singular components is done once for all.

The paper is organized as follows. In Section 2 the problem is outlined, together with the description of the polar grid discretization. The chosen basis keeps the rotational invariance of the point spread function and this leads to the block circulant structure of the coefficient matrix. In Section 3 matrix A is reduced into block diagonal form. Each block shows a further structure which allows a computational reduction. Section 4 contains a detailed description of the algorithm. The computational cost is given. Numerical experiments follow in Section 5.

2 The problem

Let $f(P)$ be the emission function to be reconstructed from the data acquired by the detectors. This function is defined on a plane domain $\varOmega$, then its values are generally represented in a grayscale image. We assume that $\varOmega$ is a disk of radius $r > 0$, centered at the origin. The detectors are aligned on a line segment $\mathcal{L}$ rotating at a constant distance from the origin. Each detector is referred by the pair of coordinates (s, θ), s being the position on $\mathcal{L}$ and θ the angle of $\mathcal{L}$ with a fixed direction. Let $g(s, \theta)$ indicate the emission from the whole object measured by the detector in (s, θ) position. A commonly accepted model for the function g is

$$g(s, \theta) = \int_{\varOmega} \mathcal{F}(s, \theta, P)\ f(P)\ dP, \tag{1}$$

where the kernel $\mathcal{F}$ represents the point spread function (PSF) of the system. In the SPECT literature there is a wide choice of PSFs. One of the most used is a 2D Gaussian PSF modified in order to take into account the dependence on the distance $d(P,\theta)$ between the point P and $\mathcal{L}$. We have

$$d(P,\theta) = r + P\cdot\boldsymbol{\theta}^{\perp}, \quad \text{where} \quad \boldsymbol{\theta}^{\perp} = (\cos\theta,\sin\theta)^{\perp} = (-\sin\theta,\cos\theta)$$

and $\cdot$ represents the scalar product between vectors. The standard deviation of the PSF is assumed to depend in a linear way on $d(P,\theta)$ as follows

$$\sigma(P) = \sigma_{\min} + \frac{\sigma_{\max}-\sigma_{\min}}{2r}\, d(P,\theta),$$

$\sigma_{\min}, \sigma_{\max}$ being given constants.

Therefore we use

$$\mathcal{F}(s,\theta,P) = \frac{1}{\sigma(P)\sqrt{2\pi}}\ \exp\Big[-\frac{(s-\widetilde{s}\,)^2}{2\sigma^2(P)}\Big], \quad \text{where} \quad \widetilde{s} = P\cdot\boldsymbol{\theta}. \tag{2}$$

The data of the problem are the values of $g(s,\theta)$ measured by the device in correspondence to a discrete set of positions (bins) s_j, $j=1,\ldots,q$ of the detectors on $\mathcal{L}$ and to a discrete set of angles θ_k, $k=0,\ldots,p-1$ of $\mathcal{L}$. We assume that p and q are even integers and that both the bins and the angles are equally spaced, that is $s_j = s_1+(j-1)\Delta s$, with $s_1=-s_q$, and $\theta_k = k\Delta\theta$, with $\Delta\theta = 2\pi/p$.

Then

$$g(s_j,\theta_k) = \int_{\Omega} \mathcal{F}(s_j,\theta_k,P)\ f(P)\ dP. \tag{3}$$

Following [2] we consider a set of linearly independent functions $\{\Phi_n(P)\}_{n=1,\ldots,N}$, called NP basis, and look for a solution of problem (1) of the form

$$f(P) = \sum_{n=1}^{N} c_n\ \Phi_n(P). \tag{4}$$

For (3) the coefficients c_n satisfy the linear system

$$g(s_j,\theta_k) = \sum_{n=1}^{N} c_n \int_{\Omega} \mathcal{F}(s_j,\theta_k,P)\ \Phi_n(P)\ dP. \tag{5}$$

System (5) constitues the so called *semidiscrete version* of problem (1).

A straightforward choice for functions $\Phi_n(P)$ is the set of the same functions $\mathcal{F}(s_j,\theta_k,P)$ used in the kernel of (3). In this way system (5) results to be square and its coefficient matrix is a symmetric Gram matrix, which turns out to be block circulant, with highly structured blocks [3].

We want to examine here a different choice of the basis. We consider on Ω a polar grid

$$\mathcal{S}_{\Omega} = \{P_{j,k} = (r_j,\theta_k),\ j=1,\ldots,q,\ k=0,\ldots,p-1\}$$

centered in the center of Ω, where the angles are the same θ_k of the measured projections and the radii r_j are selected in such a way that all the segments of circular corona have the same area α. In this way Ω results decomposed in $p \cdot q$ pixels having the shape of segments of a circular corona, the (j,k)th pixel $p_{j,k}$ being centered in $P_{j,k}$. The (j,k)th function of the NP basis is the characteristic function of the (j,k)th pixel. With this choice the coefficients of (5) are given by the integrals

$$a_{j,j'}^{(k,k')} = \int_{p_{j',k'}} \mathcal{F}(s_j, \theta_k, P)\, dP.$$

Thus system (5) results to be

$$g(s_j, \theta_k) = \sum_{j',k'} a_{j,j'}^{(k,k')}\, c_{j',k'}, \quad j, j' = 1, \ldots, q, \quad k, k' = 0, \ldots, p-1. \tag{6}$$

Due to the smooth behaviour of function $\mathcal{F}$ and to the small size of the pixels, we feel confident that the approximation

$$a_{j,j'}^{(k,k')} \sim \alpha \mathcal{F}(s_j, \theta_k, P_{j',k'}) \tag{7}$$

is acceptable and we assume $f(P) = c_{j',k'}$ for any $P \in p_{j',k'}$. System (6) with coefficients (7) becomes

$$g(s_j, \theta_k) = \alpha \sum_{P \in \mathcal{S}_\Omega} \mathcal{F}(s_j, \theta_k, P)\, f(P), \tag{8}$$

which appears to be a discrete version of (3).

Let $\mathcal{I}$ be the set of pairs of indices, ordered lexicographically in such a way that the mth entry of $\mathcal{I}$ is (j,k) with $m = kq + j$. Let $\boldsymbol{g}$ and $\boldsymbol{c}$ be the vectors whose elements are the values $g(s_j, \theta_k)$ and $c_{j,k}$ respectively. The order of the elements of the two vectors is induced by the order of $\mathcal{I}$. System (8) can be written as

$$\boldsymbol{g} = A\boldsymbol{c}, \tag{9}$$

where the (m, m') entry of matrix A is given by

$$a_{m,m'} = \alpha\, \mathcal{F}(s_j, \theta_k, P), \quad \text{where} \quad \begin{aligned} P &= (r_{j'} \cos\theta_{k'}, r_{j'} \sin\theta_{k'}), \\ m &= kp + j, \ m' = k'p + j'. \end{aligned} \tag{10}$$

The size of A, $\boldsymbol{g}$ and $\boldsymbol{c}$ is $N = pq$. The dependance of A on four indices leads to a natural partitioning in square blocks of size q, that is

$$A = \begin{bmatrix} A_{0,0} & A_{0,1} & \ldots & A_{0,p} \\ A_{1,0} & A_{1,1} & \ldots & A_{1,p} \\ \vdots & \vdots & & \vdots \\ A_{p,0} & A_{p,1} & \ldots & A_{p,p} \end{bmatrix},$$

where the (j, j') entry of block $A_{k,k'}$ is $a_{m,m'}$ defined in (10).

In order to study the structure of matrix A, we examine the properties of function $\mathcal{F}$. Let

$$U = \begin{bmatrix} \cos\Delta\theta & \sin\Delta\theta \\ -\sin\Delta\theta & \cos\Delta\theta \end{bmatrix}$$

be the unitary rotational operator. It verifies $PU\cdot\boldsymbol{\theta}_{k+1} = P\cdot\boldsymbol{\theta}_k$ and $PU\cdot\boldsymbol{\theta}_{k+1}^\perp = P\cdot\boldsymbol{\theta}_k^\perp$. Then

$$\mathcal{F}(s_j, \theta_{k+1}, PU) = \mathcal{F}(s_j, \theta_k, P).$$

It follows that

$$A_{k+1,0} = A_{k,p} \quad \text{and} \quad A_{k+1,k'+1} = A_{k,k'} \quad \text{for} \quad k, k' = 0, \dots, p-1.$$

Hence matrix A is block circulant, that is

$$A = \begin{bmatrix} A_0 & A_1 & A_2 & \dots & A_{p-1} \\ A_{p-1} & A_0 & A_1 & \ddots & \\ \vdots & \ddots & \ddots & \ddots & \\ \vdots & & \ddots & \ddots & A_1 \\ A_1 & A_2 & \dots & A_{p-1} & A_0 \end{bmatrix}, \quad \text{where} \quad A_k = A_{0,k}.$$

The (j, j') element of the block A_k is

$$a_{j,j'}^{(k)} = \alpha\,\mathcal{F}(s_j, \theta_0, P), \quad \text{where} \quad P = (r_{j'}\cos\theta_k, r_{j'}\sin\theta_k). \tag{11}$$

Moreover, for the reflection operator

$$V = \begin{bmatrix} -1 & 0 \\ 0 & 1 \end{bmatrix}$$

we have

$$\mathcal{F}(s_j, \theta_0, P) = \mathcal{F}(-s_j, \theta_0, PV).$$

Then

$$\begin{aligned} A_k &= J_q A_{p/2-k}, \quad \text{for} \quad k = 0, \dots, p/2, \\ A_{p/2+k} &= J_q A_{p-k}, \quad \text{for} \quad k = 1, \dots, p/2-1, \end{aligned} \tag{12}$$

where J_q is the reversion matrix of size q. Hence only half of the blocks of the first line of A must be constructed, namely $A_0, \dots, A_{p'}, A_{p/2+1}, \dots, A_{p/2+p'}$, where $p' = \lfloor p/4 \rfloor$. The remaining ones are obtained by reversing the lines, as shown here in the case $p = 8$

$$\begin{bmatrix} A_0 & A_1 & A_2 & JA_1 & JA_0 & A_5 & A_6 & JA_5 \end{bmatrix}$$

Note that when p is a multiple of 4 it is $A_{p/4} = JA_{p/4}$ and $A_{3p/4} = JA_{3p/4}$.

3 Exploiting the structure of A

It is well known that the $N \times N$ matrix A can be block diagonalized by means of the matrix $F_p \otimes I_q$, where I_q is the identity matrix of size q and F_p is the Fourier matrix of size p whose elements are $f_{i,j} = \omega^{ij}/\sqrt{p}$, for $i,\ j = 0, \ldots, p-1$, with $\omega = \exp(\boldsymbol{i}\, 2\pi/p)$. Then

$$A = (F_p \otimes I_q) D (F_p^H \otimes I_q), \tag{13}$$

where D is the block diagonal matrix

$$D = \begin{bmatrix} D_0 & & & \\ & D_1 & & \\ & & \ddots & \\ & & & D_{p-1} \end{bmatrix}, \quad \text{with} \quad D_k = \sum_{t=0}^{p-1} \omega^{kt} A_t. \tag{14}$$

The best way to compute the $q \times q$ blocks D_k is to make use of a fast Fourier transform. We now examine the structure of the blocks D_k. Since the blocks A_t are real, then D_0 and $D_{p/2}$ are real and

$$D_{p-k} = \overline{D}_k, \quad \text{for} \quad k = 1, \ldots, p/2 - 1.$$

Moreover from (12) it follows that

$$\begin{aligned} JD_k &= \sum_{t=0}^{p-1} \omega^{kt} JA_t = \sum_{t=0}^{p/2} \omega^{kt} JA_t + \sum_{t=p/2+1}^{p-1} \omega^{kt} JA_t \\ &= \sum_{t=0}^{p/2} \omega^{kt} A_{p/2-t} + \sum_{t=p/2+1}^{p-1} \omega^{kt} A_{3p/2-t} \\ &= \sum_{t=0}^{p/2} \omega^{(p/2-t)k} A_t + \sum_{t=p/2+1}^{p-1} \omega^{(3p/2-t)k} A_t \\ &= (-1)^k \sum_{t=0}^{p-1} \overline{\omega}^{kt} A_t = (-1)^k \overline{D}_k. \end{aligned} \tag{15}$$

By using (13), system (9) becomes

$$D\, \boldsymbol{x} = \boldsymbol{d}, \quad \text{where} \quad \boldsymbol{d} = (F_p^H \otimes I_q)\, \boldsymbol{g}, \quad \boldsymbol{x} = (F_p^H \otimes I_q)\, \boldsymbol{c}. \tag{16}$$

By partitioning vectors $\boldsymbol{x}$ and $\boldsymbol{d}$ into p subvectors of length q, system (16) decomposes into the p independent systems

$$D_k\, \boldsymbol{x}_k = \boldsymbol{d}_k, \quad \text{for} \quad k = 0, \ldots, p-1. \tag{17}$$

Since $\boldsymbol{d}_{p-k} = \overline{\boldsymbol{d}}_k$ for $k = 1, \ldots, p/2 - 1$, only the systems corresponding to indices $k = 0, \ldots, p/2$ must be solved: in fact, a system with index $k > p/2$ is the conjugate of the system with index $p - k$.

From (15) it follows that the kth system (17) can be written in the form

$$\begin{bmatrix} C_k \\ (-1)^k J_{q/2}\overline{C}_k \end{bmatrix} \boldsymbol{x}_k = \begin{bmatrix} \boldsymbol{d}_{k,1} \\ \boldsymbol{d}_{k,2} \end{bmatrix}. \tag{18}$$

For $k = 0$ and $k = p/2$ system (18) is real, with rank not greater than $q/2$. For $k = 1, \ldots, p/2-1$ system (18) is in general not real. By writing all the involved quantities as sums of a real part and an imaginary part, that is

$$C_k = C_k^{(r)} + \boldsymbol{i}\, C_k^{(i)}, \quad \boldsymbol{x}_k = \boldsymbol{x}_k^{(r)} + \boldsymbol{i}\, \boldsymbol{x}_k^{(i)}, \quad \boldsymbol{d}_{k,j} = \boldsymbol{d}_{k,j}^{(r)} + \boldsymbol{i}\, \boldsymbol{d}_{k,j}^{(i)},$$

we find that system (18) is equivalent to

$$B_k\, \boldsymbol{y}_k = \boldsymbol{b}_k, \quad \text{where} \quad B_k = \begin{bmatrix} C_k^{(r)} \\ C_k^{(i)} \end{bmatrix}, \quad \boldsymbol{y}_k = \begin{bmatrix} \boldsymbol{x}_k^{(r)} & \boldsymbol{x}_k^{(i)} \end{bmatrix}, \tag{19}$$

$$\boldsymbol{b}_k = \frac{1}{2} \begin{bmatrix} \boldsymbol{d}_{k,1}^{(r)} + (-1)^k J_{q/2}\boldsymbol{d}_{k,2}^{(r)} & \boldsymbol{d}_{k,1}^{(i)} + (-1)^k J_{q/2}\boldsymbol{d}_{k,2}^{(i)} \\ \boldsymbol{d}_{k,1}^{(i)} - (-1)^k J_{q/2}\boldsymbol{d}_{k,2}^{(i)} & -\boldsymbol{d}_{k,1}^{(r)} + (-1)^k J_{q/2}\boldsymbol{d}_{k,2}^{(r)} \end{bmatrix}.$$

We note that

$$D_k = S\, B_k, \quad \text{where} \quad S = \begin{bmatrix} I_{q/2} & \boldsymbol{i} I_{q/2} \\ (-1)^k J_{q/2} & -\boldsymbol{i}(-1)^k J_{q/2} \end{bmatrix}.$$

Since $S^H S = 2I_q$, the singular values of D_k and B_k are the same, apart the factor $\sqrt{2}$.

4 The algorithm

In the kind of application we are considering, many systems of the form (9) have to be solved, with the same coefficient matrix and different vectors $\boldsymbol{g}$. Hence it is convenient to perform once for all a preprocessing phase on matrix A. Then a reconstruction phase of the emission function $\boldsymbol{c}$ for any new input data $\boldsymbol{g}$ is performed. In this way the most relevant part of the computational burden is placed in the preprocessing stage.

Since we are interested into computing a regularized solution, we choose the truncated SVD method. The SVD decomposition of matrices B_k for $k = 0, \ldots, p/2$ is computed. A suitable threshold value ϵ is defined and the singular values $\sigma_i^{(k)} > \epsilon$ are considered, together with the corresponding singular vectors $\boldsymbol{u}_i^{(k)}$ and $\boldsymbol{v}_i^{(k)}$. We note that the singular values of the matrices B_k tend to decrease when index k increases from 0 to $p/2$.

The algorithm is composed of two phases:

(a) a preprocessing phase, where the required singular components are computed,

(b) a reconstruction phase where the vector $\mathbf{g}$ of the measured data is processed.

Of course only the second phase is required for any new data vector.

4.1 (a) - Preprocessing phase

1 - For any $j = 1, \dots, q/2$ and $j' = 1, \dots, q$ compute the values

$$a_{j,j'}^{(k)}, \quad k = 0, \dots, p' \text{ and } k = p/2+1, \dots, p/2+p', \text{ where } p' = \lfloor p/4 \rfloor$$

from (11). Complete the vector $\boldsymbol{w} = [a_{j,j'}^{(k)},\ k = 0, \dots, p-1]$ with the elements

$$\begin{aligned} a_{j,j'}^{(k)} &= a_{j,j'}^{(p/2-k)}, \quad k = p'+1, \dots, p/2, \\ a_{j,j'}^{(k)} &= a_{j,j'}^{(3p/2-k)}, \quad k = p/2+p'+1, \dots, p-1. \end{aligned}$$

Compute $\boldsymbol{z} = \sqrt{p}\, DFT(\boldsymbol{w})$ and store

$$(B_k)_{j,j'} = z_k^{(r)}, \quad (B_k)_{p/2+j,j'} = z_k^{(i)}, \quad k = 0, \dots, p/2.$$

2 - Let ϵ be the threshold value for truncated SVD. For $k = 0, \dots, p/2$ compute the singular value decomposition of B_k. Let n_k be the number of the singular values $\sigma_i^{(k)}$ greater than ϵ. Store $\sigma_i^{(k)}$ and the corresponding singular vectors $\boldsymbol{u}_i^{(k)}$ and $\boldsymbol{v}_i^{(k)}$ for $i = 1, \dots, n_k$.

4.2 (b) - Reconstruction phase

3 - For $j = 1, \dots, q$ let $\boldsymbol{w}$ be the vector of entries $w_k = g(s_j, \theta_k)$, $k = 0, \dots, p-1$. Compute $\boldsymbol{z} = IDFT(\boldsymbol{w})$ and store $d_j^{(k)} = z_k$, $k = 0, \dots, p-1$.

4 - For $k = 0, \dots, p/2$ compute $\boldsymbol{b}_k$ according to (19). Apply the truncated SVD to system (19), that is compute

$$\boldsymbol{y}_k = \sum_{i=1}^{n_k} \frac{1}{\sigma_i^{(k)}} \boldsymbol{v}_i^{(k)} \boldsymbol{u}_i^{(k)T} \boldsymbol{b}_k.$$

The real and imaginary part of $\boldsymbol{x}_k$ are the two columns of $\boldsymbol{y}_k$. Join all the vectors $\boldsymbol{x}_k$ into vector $\boldsymbol{x}$.

5 - For $j = 1, \dots, q$ let $\boldsymbol{w}$ be the vector of entries $w_k = x_{kq+j}$, $k = 0, \dots, p-1$. Compute $\boldsymbol{z} = DFT(\boldsymbol{w})$ and store $c_{kq+j} = z_k$, $k = 0, \dots, p-1$.

We have thus computed the reconstructed image $\boldsymbol{c}$ on the polar grid. As it is customary, the negative values of $\boldsymbol{c}$ should be set to zero.

4.3 Computational costs

For step 1 we consider the cost of computing $q^2/2$ Fourier transforms of length p. For stop 2 the computation of the $p/2+1$ singular values decompositions has a cost $O(pq^3)$ [7]. Hence the complexity of the preprocessing phase is $O(pq^3 + q^2 p \log p)$. In the real case p and q are comparable, then the preprocessing has the cost $O(p^4)$.

Assuming that the singular values selected by the chosen ϵ are m, the cost of step 4 is $O(qm)$. For steps 3 and 5 we consider the cost of computing $2q$ Fourier transforms of length p. Hence the complexity of the reconstruction phase is $O(qm + qp \log p)$. If m is comparable with $p \log p$ (the experiments show that with such values of m acceptable reconstructed images are obtained) the cost of the reconstruction phase is $O(p^2 \log p)$.

5 Numerical experimentation

We simulate a reconstruction process by using synthetic data obtained from the 128×128 pixel image of a slice of the Hoffman brain phantom [8] (see Figure 1). From this image the values of $\boldsymbol{c}$ have been interpolated on a polar

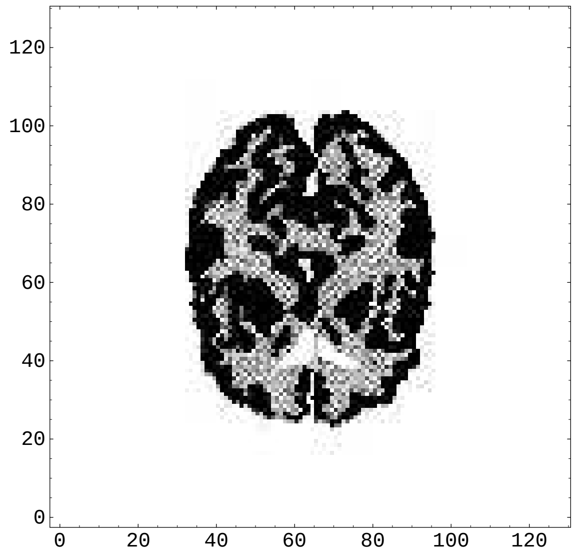

Figure 1: Original image.

grid. The values we have used for the constants are customary for this kind of device: $r = 192$, $p = 120$, $q = 128$, $\Delta s = 3$, $s_{\min} = 3$, $s_{\max} = 8$ (all expressed in mm). The values of the vector $\boldsymbol{s} = A\boldsymbol{c}$ have been computed and rounded to nearest integer. Then a Poisson noise has been added. The threshold value ϵ for truncated SVD has been determined experimentally, by comparing the reconstructions with the original image. The reconstructed image obtained from the algorithm is in polar coordinates and has been converted into Cartesian coordinates for displaying. It could be displayed directly in polar pixel through a suitable graphic tool.

Figure 2 shows the reconstructed image with singular values greater than 0.04 (19% of the total) when normalized noise of size 10^{-3} has been added. Figure 3 shows the reconstructed image with singular values greater than 0.03 (13% of the total) when normalized noise of size 10^{-2} has been added.

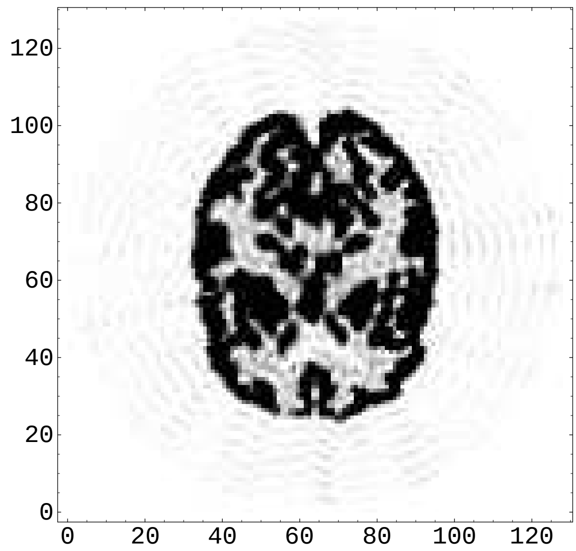

Figure 2: Reconstructed image with 19% singular values.

References

[1] M. Bertero, P. Boccacci, *Introduction to Inverse Problems in Imaging*, Institute of Physics Publishing, 1998.

[2] M. Bertero, C. De Mol and E. R. Pike, Linear inverse problems with discrete data. 1: General formulation and singular system analisys, *Inverse Problems* 1 (1985) 301-330.

[3] R. Bevilacqua, E. Bozzo and O. Menchi, SPECT imaging reconstruction: Proposal of an algorithm which exploits the matrix structure, *Technical Report* TR-01-12, Dipartimento di Informatica, Università di Pisa, 2001.

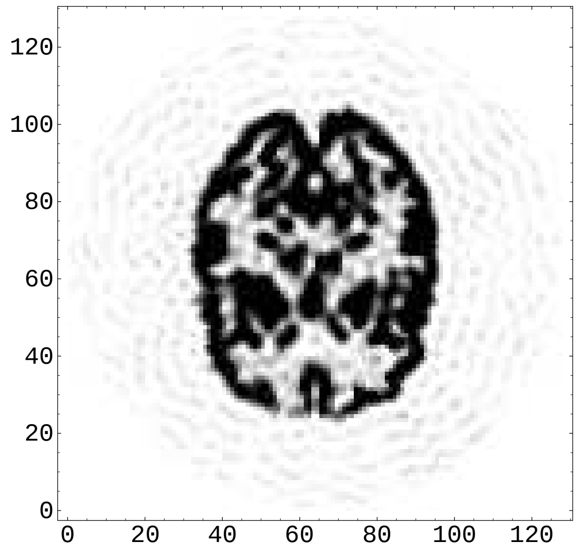

Figure 3: Reconstructed image with 13% singular values.

[4] D. Bindi, P. Brianzi, F. Di Benedetto, *A Fourier Approach to the Natural Pixel Discretization of Brain Single-Photon Emission Computed Tomography*, Int. J. of Imaging Syst. and Technol. 12-1 (2002) 1-8.

[5] P. Boccacci, P. Bonetto, P. Brianzi, P. Calvini, F. Di Benedetto, A. R. Formiconi, A. Passeri, *The 2D+1 method for an Efficient Modelling of Collimator Blur in 3D SPECT imaging*, Ann. Univ. Ferrara, Sez. VII - Sc. Mat. Suppl. Vol. XIV (2000).

[6] P. Brianzi, F. Di Benedetto, *Exploiting Matrix Structures in SPECT models*, to appear in "Structured Matrices: Recent Developments in Theory and Computation", D. Bini, E. Tyrtyshnikov and P. Yalamov eds., Nova Science Publisher Inc., New York, 2000.

[7] G.H. Golub, C.F. Van Loan, *Matrix Computation*, 2nd ed. Johns Hopkins University Press, Baltimore 1989.

[8] E.J. Hoffman, P.D. Cutler, W.M. Digby, J.C. Mazziotta, 3-D phantom to simulate cerebral blood flow and metabolic images for PET, *IEEE Trans. Nucl. Sci.*, 37: 616-620 (1990).